Published OnlineFirst January 13, 2020; DOI: 10.1158/1078-0432.CCR-19-1954

A Small Hypoxia Signature Predicted pCR Response to Bevacizumab in the Neoadjuvant GeparQuinto Breast Cancer Trial

Thomas Karn[1], Tobias Meissner[2], Karsten E. Weber[3], Christine Solbach[1], Carsten Denkert[4], Knut Engels[1], Peter A. Fasching[5], Bruno V. Sinn[4], Iris Schrader[6], Jan Budczies[4], Frederik Marmé[7], Volkmar Müller[8], Uwe Holtrich[1], Bernd Gerber[9], Christian Schem[10], Brandon M. Young[2], Claus Hanusch[11], Elmar Stickeler[12], Jens Huober[13], Marion van Mackelenbergh[14], Brian Leyland-Jones[2], Tanja Fehm[15], Valentina Nekljudova[3], Michael Untch[16], and Sibylle Loibl[3]

ABSTRACT

Purpose: In breast cancer, bevacizumab increased pCR rate but not long-term survival and no predictive markers are available to identify patients with long-term benefit from the drug.

Experimental design: We profiled 289 pretherapeutic formalin-fixed, paraffin-embedded (FFPE) biopsies of HER2-negative patients from the GeparQuinto trial of neoadjuvant chemotherapy ± bevacizumab by exome-capture RNA-sequencing (RNA-seq). In a prospectively planned study, we tested molecular signatures for response prediction. IHC validation was performed using tissue microarrays.

Results: We found strong agreement of molecular and pathologic parameters as hormone receptors, grading, and lymphocyte infiltration in 221 high-quality samples. Response rates (49.3% pCR overall) were higher in basal-like (68.9%) and HER2-enriched (45.5%) than in luminal B (35.7%), luminal A (17.9%), and normal-like (20.0%) subtypes. T-cell (OR = 1.60; 95% confidence interval, 1.21–2.12; $P = 0.001$), proliferation (OR = 2.88; 95% CI, 2.00–4.15; $P < 0.001$), and hypoxia signatures (OR = 1.92; 95% CI, 1.41–2.60; $P < 0.001$) significantly predicted pCR in univariate analysis. In a prespecified multivariate logistic regression, a small hypoxia signature predicted pCR (OR = 2.40; 95% CI, 1.28–4.51; $P = 0.006$) with a significant interaction with bevacizumab treatment ($P = 0.020$). IHC validation using NDRG1 as marker revealed highly heterogenous expression within tissue leading to profound loss of sensitivity in TMA analysis, still a significant predictive value for pCR was detected ($P = 0.025$).

Conclusions: Exome-capture RNA-seq characterizes small FFPE core biopsies by reliably detecting factors as for example ER status, grade, and tumor-infiltrating lymphocytes levels. Beside molecular subtypes and immune signatures, a small hypoxia signature predicted pCR to bevacizumab, which could be validated by IHC. The signature can have important applications for bevacizumab treatment in different cancer types and might also have a role for novel combination therapies of bevacizumab with immune checkpoint inhibition.

Introduction

Adding bevacizumab to neoadjuvant chemotherapy in breast cancer increases pCR rates (1–4), but this difference in response did not translate into a robust improvement of survival (5–8). Several explanations for this paradox have been proposed, including a greater effect of bevacizumab on vascularization of primary tumors than on micrometastases (6, 9). Nevertheless, patient subsets with long-term benefit from bevacizumab may exist, but despite considerable efforts no robust predictive markers are available to identify them (10, 11). Still, in several other solid cancer types bevacizumab currently has an important clinical role (12). Moreover, new combination therapies of bevacizumab with immune checkpoint inhibitors show promising results (13–16).

Molecular subtypes of breast cancer differ in prognosis and treatment response. We previously demonstrated that in TNBC lymphocyte signatures correlate with good prognosis and response to neoadjuvant chemotherapy, whereas hypoxia/inflammatory signatures (VEGFA/IL8 metagenes) are associated with poor prognosis (17, 18). On the other hand, hypoxia is an important regulator of VEGF (11). Therefore, it may be hypothesized that tumors with hypoxia could be more dependent on VEGF and responsive to its inhibition. Thus, hypoxia signatures may be candidate markers to predict response to bevacizumab treatment. Another simplistic model may be that hypoxia and necrosis signatures might characterize tumors that are already "knocked on," and such tumors could show increased response to

[1]Goethe University Hospital Frankfurt, Frankfurt, Germany. [2]Avera Cancer Institute, Sioux Falls, South Dakota. [3]German Breast Group, Neu-Isenburg, Germany. [4]Charite Berlin, Berlin, Germany. [5]Department of Gynecology and Obstetrics, University Hospital Erlangen, Comprehensive Cancer Center Erlangen-EMN, Friedrich-Alexander University Erlangen-Nuremberg, Germany. [6]Gynäkologisch-Onkologische Praxis Hannover, Hannover, Germany. [7]University Hospital Heidelberg, Heidelberg, Germany. [8]University Hospital Hamburg-Eppendorf, Hamburg-Eppendorf, Germany. [9]University Hospital Rostock, Rostock, Germany. [10]Mammazentrum Hamburg, Hamburg, Germany. [11]Rotkreuzklinikum München, München, Germany. [12]University Hospital Aachen, Aachen, Germany. [13]University Hospital Ulm, Ulm, Germany. [14]University Hospital Schleswig-Holstein, Kiel, Germany. [15]University Hospital Tübingen, Tübingen, Germany. [16]Helios Kliniken Berlin-Buch, Berlin, Germany.

Note: Supplementary data for this article are available at Clinical Cancer Research Online (http://clincancerres.aacrjournals.org/).

Current address for Jan Budczies: University Hospital Heidelberg, Heidelberg, Germany; current address for Frederik Marmé: University Hospital Mannheim, Mannheim, Germany; current address for Carsten Denkert: University of Marburg, Germany.

Corresponding Author: Thomas Karn, Goethe University Hospital Frankfurt, Theodor-Stern-Kai 7, Frankfurt 60590, Germany. Phone: 496963014120; Fax: 496963017025; E-mail: t.karn@em.uni-frankfurt.de

Clin Cancer Res 2020;XX:XX–XX

doi: 10.1158/1078-0432.CCR-19-1954

Published OnlineFirst January 13, 2020; DOI: 10.1158/1078-0432.CCR-19-1954

Translational Relevance

In this prospectively planned study, we tested molecular signatures for response prediction to neoadjuvant chemotherapy ± bevacizumab in the GeparQuinto breast cancer trial. To this end, we profiled pretherapeutic FFPE biopsies by exome-capture RNA-seq. Beside molecular subtypes and immune signatures, a small hypoxia signature predicted pathologic complete response. This signature was validated by IHC and can have important applications for bevacizumab treatment in different cancer types and might also have a role for novel combination therapies of bevacizumab with immune checkpoint inhibition.

different kinds of treatment. Although molecular profiling of partially degraded RNA from archival FFPE tissues had been challenging, recently developed new exome capture RNA-seq methods show some promising results (19, 20). Therefore, the goal of the present blinded study was to profile pretreatment FFPE biopsies of HER2-negative breast cancers from the neoadjuvant GeparQuinto trial (1, 6) by this method, to identify a predictive marker for response to bevacizumab treatment. We analyzed robustness of the methodology and followed a prespecified protocol to test molecular subtypes, T-cell and hypoxia signature as predictors of response. We found that the hypoxia signature specifically predicts pCR to bevacizumab treatment and identified NDRG1 IHC as a single marker for signature validation.

Materials and Methods

All analyses were performed according to the "REporting recommendations for tumor MARKer prognostic studies" (REMARK) criteria (21) with a "prospective-retrospective" design (22). A CONSORT type diagram (23) of the flow of samples through the study is shown in Supplementary Fig. S1.

Patients

The details of the GeparQuinto trial (NCT 00567554) have been described in several previous publications (1, 6). In this study, only HER2-negative patients from GeparQuinto were included. These patients were treated with anthracycline and taxane neoadjuvant chemotherapy and were randomly assigned to either simultaneous treatment with bevacizumab or no additional therapy. In total, 1,948 patients were randomly assigned in the main study. This study is based on 1540 HER2-negative patients with response data (Supplementary Fig. S1). The biomarker investigations were conducted in accordance with the International Ethical Guidelines for Biomedical Research involving Human Subjects (CIOMS). Written informed consent for use of biomaterials was obtained from all patients, ethic committee approval was obtained for all centers participating in the clinical study and from the institutional review board of the Charité Hospital.

Statistical analysis plan of preplanned blinded study

The statistical analysis plan (SAP) of this project was finalized at 2016-01-28. Analysis teams were fully blinded to either molecular or clinical data, respectively. The specific roles and blinding status of all contributing teams is given in Supplementary Table S1. The predefined analytical aims of the study are presented in Supplementary Table S2.

Tissue samples

Formalin-fixed paraffin embedded (FFPE) tissue of pretherapeutic cores with written informed consent were stored in the GBG tumor bank at the Institute of Pathology, Charité Hospital, Berlin, Germany. All available tissue samples from HER2-negative patients with pCR ($N = 181$) were selected and $n = 197$ samples of non-pCR patients were chosen randomly to have 378 samples overall (Supplementary Fig. S1).

RNA-seq profiling and primary bioinformatic analysis

For RNA extraction, 5 μm FFPE sections were deparaffinized, RNA extracted using *RecoverAll FFPE* Kit (Ambion/Invitrogen), DNase treated, and purified using AMPure RNA XP Clean beads (Agencourt Bioscience Corp.). Samples with <40 ng RNA were excluded from further analysis. RNA-seq from total RNA in FFPE tissue can be challenging due to limited capture of partially degraded RNA (24). In contrast, exome-capture–based RNA-seq may allow reproducible molecular characterization of such low-quality RNA (19, 20, 25, 26). We used the Illumina TruSeq RNA Access Library Prep Kit (Illumina) with 40 ng of FFPE RNA. Libraries were processed in batches of 48 and 12 samples were pooled per multiplex sequencing run, clustered onto a NextSeq 500 High Output flow cell, and sequenced to either 150 or 75 bp paired end reads. For samples that failed initial QC based on post PCR yield (<3.5 ng) or missing reads for one of 18 housekeeping genes (*ABCF1, ACTB, ALAS1, B2M, CLTC, G6PD, GAPDH, GUSB, HPRT1, LDHA, PGK1, POLR1B, POLR2A, RPL19, RPLP0, SDHA, TBP, TUBB*), library generation was repeated. All sequence data were processed using Omics Pipe (27). FastQC (v0.11.2) was used for read quality check, BBDuk (v34.46) for adapter trimming (with parameters: *minlen = 25 qtrim = rl trimq = 10 ktrim = r k = 25 mink = 11 hdist = 1 overwrite = true tbo = t tpe = t*), STAR (v2.4.0g1) for alignment to hg19 (28), SAMtools (v0.1.19) for sorting, and featureCounts (v1.4.6) using Refseq hg19 for gene counts (29). Samples with less than 3 million total raw reads, or with less than one count in the set of 18 control genes, were marked as low quality. RNA-seq data of 289 patients were classified as either of high ($N = 221$) or of low quality ($N = 68$) as shown in Supplementary Fig. S1. The final blinded RNA-seq dataset was transferred to GBG-headquarter and distributed to analysis teams. A comparison of the complete trial cohort and the RNA-seq cohorts is provided in Supplementary Table S3. The analysis of the RNA-seq dataset was performed fully blinded to any clinical or pathologic sample information.

Concordance of ER and PR status and molecular subtyping

Cutoffs for RNA-seq–derived ER and PR status were based on the bimodal distribution of variance stabilized count data (30) of the two genes. Concordance with pathologic classification was analyzed as described previously (31). The "Absolute Intrinsic Molecular Subtypes (AIMS)" method, which is independent of dataset composition (32), was applied as a single sample predictor using raw count data. Of all 23,710 genes in the RNA-seq dataset, 19,000 were successfully linked to an EntrezID as required for the AIMS method.

Platform transfer of gene signatures

Despite the ability to detect several marker genes, the exome-capture–based RNA-seq data from FFPE clearly differed from other datasets of microarray of RNA-seq analyses from frozen tissue samples. This bias precluded a simple application of any predefined gene-lists as signatures, which were derived from different platforms. Instead, we focused in our analysis on robust expression signals (or "metagenes") that met the following criteria:

Published OnlineFirst January 13, 2020; DOI: 10.1158/1078-0432.CCR-19-1954

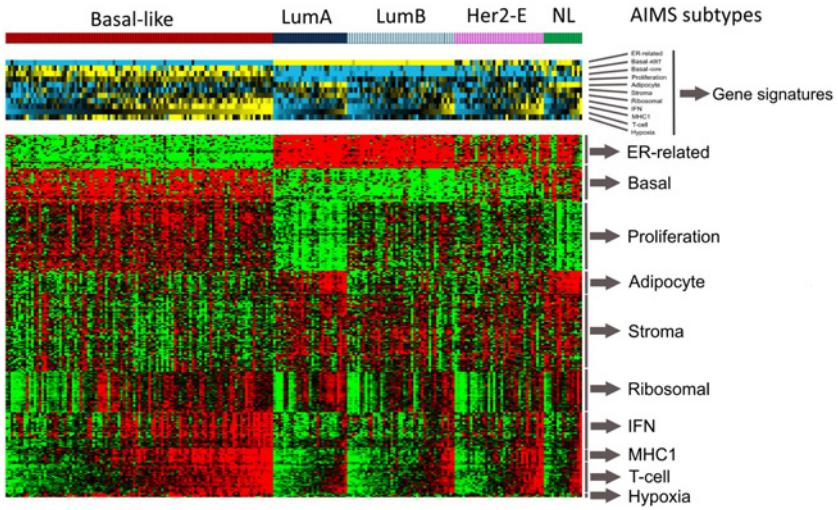

Figure 1.
Molecular subtypes and gene signatures in pretherapeutic core samples from the GeparQuinto trial. A total of 221 samples with high-quality RNA-seq data were stratified into molecular subtypes using the AIMS method, and the respective subtype classifications are given in the upmost row (Lum, luminal; HER-E: HER2-enriched; NL, normal-like). In addition, log_2 count data of 268 genes from gene clusters representing previously identified signatures from our microarray (17) and RNA-seq studies (18) were median centered and are represented in the bottom panel (red/green) heatmap. Gene signatures in the above (yellow/blue) heatmap were calculated as mean values of the respective gene clusters in the bottom panel. Samples were sorted first according to AIMS subtype and second within each subtype according to T-cell signature expression from left to right.

(i) signals need to be clearly measurable, (ii) distinguishable from each other, and (iii) principally reproducible in different datasets. Previous studies have shown that technological variability can be overcome by noise filtering combined with unsupervised hierarchical clustering, which results in overlapping, but not identical marker sets for metagenes on different platforms and datasets (refs. 17, 18, 33–38).

We used only the 221 high-quality samples to derive robust gene clusters for platform transfer. To reduce noise, a gene filter was applied requiring at least 10 read counts in more than 10% of the samples. Log_2 count data of 7,518 genes passing this filter were median centered and then used for hierarchical clustering. We then identified reproducible gene clusters representing previously identified gene signatures from our microarray (17) and RNA-seq studies (18) as metagenes for "ER-related," "Basal," "Proliferation," "Adipocytes," "Stroma," "Ribosomal," "IFN," "MHC2," "T-cell," and "Hypoxia" (**Fig. 1**). The 268 individual genes of these clusters were extracted and signatures were calculated as mean values of the respective genes and then z-transformed. Gene lists of signatures are provided in Supplementary Table S4.

IHC validation

Marker selection

The principal procedure of the approach for IHC validation is presented in Supplementary Fig. S2. The hypoxia gene cluster was previously identified in breast cancer expression data in several studies and associated with poor prognosis (17, 18, 33, 39, 40). To characterize this group of genes in more detail, we performed unsupervised cluster analyses in different cohorts and datasets of breast cancers from different platforms (Supplementary Fig. S2A). The platforms encompassed Affymetrix (17, 31), Agilent (33), Illumina (34), RNA-seq (18, 35), and FFPE-RNA-seq. The different assembled cohorts encompassed either triple negative breast cancer (TNBC) as a single subtype, cohorts of ER negative tumors (both TNBC and HER2), or both ER positive and ER negative tumors together. As a consensus cluster, we identified a stable core of six genes with correlated expression which are presented in Supplementary Table S5. All six genes are linked to hypoxia, angiogenesis, and stress response. However, the filtered FFPE RNA-seq dataset from GeparQuinto contained only measurements for 3 of the 6 genes (*VEGFA, NDRG1, CSTB*). Thus, these 3 genes were studied further for IHC validation.

IHC transfer in independent dataset

To establish an IHC assay for the signature, we first used an independent Affymetrix microarray dataset of TNBC (17). As presented in Supplementary Fig. S2A, we performed blinded IHC analysis of the three markers (VEGFA, NDRG1, CSTB) and compared IHC scorings and Affymetrix gene expression data for 26 TNBC samples (Supplementary Fig. S3). The best correlation was found for NDRG1 ($R^2 = 0.526$) with an absolute intraclass correlation (ICC) of 0.98 (95% confidence interval [CI], 0.96–0.99) between two independent observers. Moreover, IHC revealed strong para-necrotic expression of NDRG1 in line with its presumed functions in cellular stress and hypoxia (refs. 41–45; Supplementary Fig. S4).

IHC analysis of core biopsy samples from GeparQuinto

Because we observed considerable heterogeneity of expression within tissues samples, we next tested whether NDRG1 IHC can be performed on core biopsy samples from the clinical trial (Supplementary Fig. S2B). We defined a cutoff of *z*-score 1.5 from the RNA-seq data of GeparQuinto as strong expression and selected a test cohort of 27 GeparQuinto samples. Blinded visual scoring of whole slide IHC of the core biopsies was performed to assess sensitivity and specificity of classification by the pathologist compared with RNA-seq. In addition, we performed digital image analysis using QuPath software (46, 47) and analyzed sensitivity and specificity with a cutoff of 10% positive cells (Supplementary Fig. S2B). The corresponding data on accuracy are given in (Supplementary Table S6).

IHC analysis of microcore TMA

Finally, we analyzed a tissue microarray (TMA) cohort of small microcores from the core biopsies of all GeparQuinto samples with RNA-seq data using digital image analysis (Supplementary Fig. S2C). This dataset was used to validate the predictive value of NDRG1 for pCR and to study the loss of sensitivity in the TMA format because of heterogeneity in expression.

Statistical analysis

All clinical data, including estrogen and progesterone receptor status were extracted from the clinical study database at GBG headquarter and represent local assessment. For 67 of the high-quality samples tumor-infiltrating lymphocyte (TIL) scoring was available on file from the PREDICT study (48), all from the non-bevacizumab

Published OnlineFirst January 13, 2020; DOI: 10.1158/1078-0432.CCR-19-1954

group. To avoid any overfitting, all cutoffs and analysis steps were predefined in writing, blinded to any patient data. Continuous signatures for proliferation, stroma, T cells, and hypoxia were z-transformed for use in univariate and multivariate logistic regression. Pearson chi-square and Fisher exact test were applied to assess associations between categorical parameters. To analyze the predictive value of molecular markers for pCR univariate and multivariate logistic regression adjusted for relevant prespecified baseline characteristics were used. The R software environment (http://www.r-project.org/) and SPSS 24 (http://www.ibm.com/) were used for all analyses. All P values are two-sided and $P = 0.05$ was considered as significant. Supplementary information on code and data are available online at https://github.com/tkarn/G5-RNA-Seq.

Results

Molecular profiling of FFPE cores by exome-capture–based RNA-seq

Of 378 pretherapeutic biopsies from HER2-negative patients of the GeparQuinto trial, 289 samples with RNA-seq data were classified as either of high ($N = 221$) or of low quality ($N = 68$). For 54 samples, RNA yield was insufficient and 35 did not pass initial QC (Supplementary Fig. S1). A comparison of the complete HER2-negative trial cohort and the RNA-seq cohorts is provided in Supplementary Table S3. Because of the enrichment in patients with pCR in the RNA-seq cohort, we also detected a significantly higher proportion of hormone receptor negative high-grade tumors in this comparison.

To study robustness of the data, we first compared RNA-seq–derived ER and PR status of the samples with data from local pathology in a blinded fashion. IHC classifications strongly correlated with gene expression (overall correctness 84% and 81% for ER, and 81% and 75% for PR, in samples with high and low quality, respectively; Supplementary Table S7). These data may suggest that samples with low quality might still be used for basic subtype stratification despite a lower number of genes with measurable expression values. However, results from molecular subtyping differed significantly for the low-quality group and most of the gene signatures could not be effectively measured in those samples (see Supplementary Fig. S5 and Table S8). Therefore, we focused in all subsequent analyses only on the 221 high-quality samples.

We next stratified the high-quality samples into molecular subtypes by applying the AIMS method as single sample predictor (32). A total of 103 (46.6%), 33 (14.9%), 28 (12.7%), 42 (19.0%), and 15 (6.8%) samples were classified as basal-like, HER2-enriched, luminal A, luminal B, and normal-like, respectively (**Table 1**). Molecular subtypes clearly differed in ER and PR IHC-status with more than 95% hormone receptor positive tumors in the luminal groups but only 20% in the basal-like group (**Table 1**). Moreover, we found that most basal-like tumors were histologic grade 3 (80.4% compared with 18.5% of luminal A). Also the luminal B group contained more grade 3 tumors (38.1%) and a higher percentage of ER+/PR− tumors than luminal A (16.7% vs. 3.6%), which we also observed for the HER2-enriched group (15.2%, **Table 1**).

Gene signatures for additional biological phenotypes

We used the 221 high-quality samples for platform transfer of previously described gene signatures for different biological phenotypes (17, 18). **Figure 1** demonstrates the expression of 10 such signatures (ER-related, basal, proliferation, adipocyte, stroma, ribosomal, IFN, MHC1, T-cell, and hypoxia) in the different molecular subtypes. As proof of principle, we tested three signatures (proliferation, stroma, T-cell) for their association with data from histopathologic analysis. As expected, the proliferation signature correlated with histological grade (median −0.73, −0.39, and 0.53 in G1, G2, and G3, respectively; $P < 0.001$; Supplementary Fig. S6). For tumor content, we detected a weak inverse correlation with the T-cell signature (Spearman $\rho = -0.13$; $P = 0.049$), but no significant association with stroma and proliferation signatures. Scoring for TILs counts was on file for 67 of the high-quality samples in the clinical database from the PREDICT study (48). We found a strong positive correlation of TIL counts with the T-cell signature (Spearman $\rho = 0.53$; $P < 0.001$), whereas the stroma signature showed an inverse correlation (Spearman $\rho = -0.31$; $P = 0.010$), and no significant association with the proliferation signature was detected.

Molecular markers and prediction of response

To avoid overfitting, we tested a restricted predefined subset of four variables (molecular subtype and the proliferation, T cell, and hypoxia signatures) as predictors in univariate logistic regression of pCR. As shown in **Table 1**, response rates (49.3% overall in this pCR enriched cohort) differed significantly by subtype ($P < 0.001$), with higher pCR rates in basal-like (68.9%) and HER2 enriched (45.5%) than in luminal B (35.7%), luminal A (17.9%), and normal-like (20.0%). In univariate logistic regression analysis, both basal-like subtype ($P = 0.001$), T cell (OR = 1.60; 95% CI, 1.21–2.12; $P = 0.001$), proliferation (OR = 2.88; 95% CI, 2.00–4.16; $P < 0.001$), and hypoxia signatures (OR = 1.92; 95% CI, 1.41–2.60; $P < 0.001$) were significant predictors for pCR (Supplementary Table S9).

We next performed prespecified multivariate logistic regression of pCR, which included the following variables: hormone receptor status, treatment arm (±bevacizumab), the hypoxia signature, and the interaction term between the treatment arm and the hypoxia signature (model A in **Table 2**). In this analysis, both hormone receptor status

Table 1. Molecular subtyping of HER2-negative tumors from geparquinto trial by FFPE-RNA-seq.

Group Total ($N = 221$, %)	Basal-like 103 (46.6%)	HER2-enriched 33 (14.9%)	LumA 28 (12.7%)	LumB 42 (19.0%)	Normal-like 15 (6.8%)	*P* value
HR-positive (53.8%)	19.4%	66.7%	96.4%	95.2%	66.7%	<0.001
ER+/PR+ (40.7%)	7.8%	48.5%	89.3%	78.6%	53.3%	
ER+/PR− (11.3%)	9.7%	15.2%	3.6%	16.7%	13.3%	
ER−/PR+ (1.8%)	1.9%	3.0%	3.6%	0%	0%	
ER−/PR− (46.2%)	80.6%	33.3%	3.6%	4.8%	33.3%	<0.001
Grade 3 (57.5%)	80.4%	54.5%	18.5%	38.1%	33.3%	<0.001
pCR (49.3%)	68.9%	45.5%	17.9%	35.7%	20.0%	<0.001

Published OnlineFirst January 13, 2020; DOI: 10.1158/1078-0432.CCR-19-1954

Table 2. Multivariate logistic regression of pCR.

Model				Model A			Model B			Model C		
A	B	C		OR	95% CI	*P* value	OR	95% CI	*P* value	OR	95% CI	*P* value
|	|	|	Hormone receptor (neg. vs. pos.)	3.97	2.14–7.38	**<0.001**	3.50	1.78–6.89	**<0.001**	3.45	1.75–6.82	**<0.001**
|	|	|	Hypoxia signature (*z*-score)	2.59	1.40–4.76	**0.002**	2.40	1.28–4.51	**0.006**	2.17	1.14–4.10	**0.018**
|	|	|	Bevacizumab therapy	1.25	0.67–2.31	0.48	1.23	0.65–2.34	0.52	1.20	0.63–2.27	0.58
|	|	|	Interaction hypoxia signature * bevacizumab	2.29	1.12–4.69	**0.023**	2.38	1.15–4.95	**0.020**	2.35	1.14–4.85	**0.021**
	|	|	cN (≥10 vs. 4-9 vs. 1-3 vs. 0 positive nodes)				0.90	0.55–1.48	0.68	0.93	0.57–1.52	0.77
	|	|	cT (T4d vs. T4a-c vs. T3 vs. T2 vs. T1)				0.87	0.60–1.25	0.44	0.91	0.63–1.31	0.60
	|	|	Grading (G3 vs. G2 vs. G1)				1.78	0.95–3.33	0.073	1.80	0.95–3.39	0.069
		|	T-cell signature (*z*-score)							1.27	0.90–1.79	0.177

Note: Numbers in bold indicate significant *P* values.

(OR = 3.97; 95% CI, 2.14–7.38; $P < 0.001$) and the hypoxia signature (OR = 2.59; 95% CI, 1.40–4.76; $P = 0.002$) were strong predictors of pCR with a significant interaction between the hypoxia signature and the treatment arm ($P = 0.023$). In additional multivariate analysis, we included the same variables (HR, treatment, hypoxia signature, and the interaction term) as well as additional clinical parameters (lymph node status, tumor size, and grade; model B in **Table 2**) and the T-cell signature (model C in **Table 2**). As shown in **Table 2**, the hypoxia signature (OR = 2.40; 95% CI, 1.28–4.51; $P = 0.006$ and OR = 2.17; 95% CI, 1.14–4.10; $P = 0.018$, for models B and C, respectively)

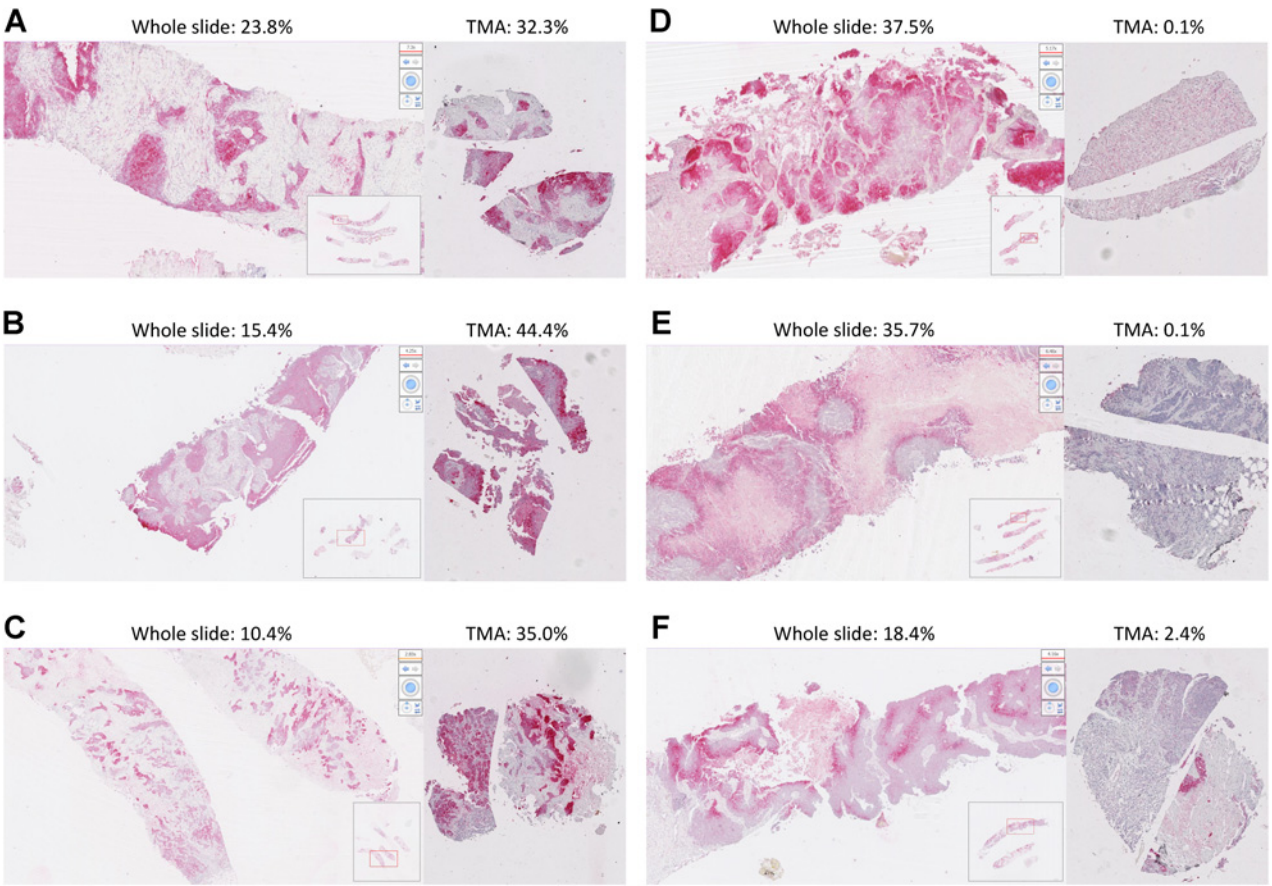

Figure 2.

Examples of loss of NDRG1 expression signal in TMA analysis. **A, B,** and **C** present three examples, where the NDRG1 expression signal is detected both in whole slide analysis and in the small TMA core of the respective sample. In contrast, **D, E,** and **F** presented three different examples, where the expression signal from whole slide analysis was lost in the TMA analysis. For each of the six samples two images are shown: the left image shows an enlarged region of the whole slide IHC (with full slide overview in the small box at the bottom). The right image shows the result of the small TMA microcore from the same sample. Percentage of positive cells from digital image analyses by QuPath are given above the respective images.

Published OnlineFirst January 13, 2020; DOI: 10.1158/1078-0432.CCR-19-1954

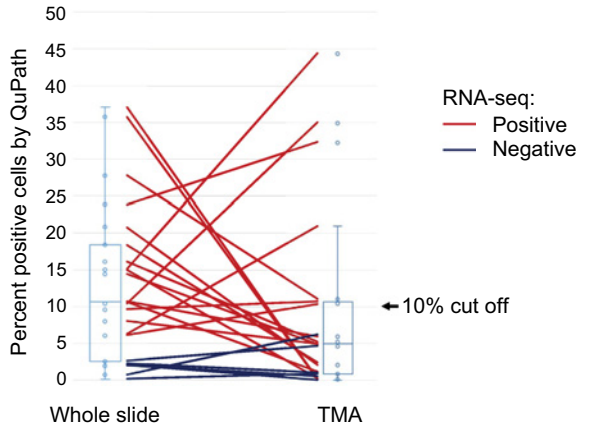

Figure 3.

Loss of NDRG1 expression signal in TMA analysis. Distribution of measurements of percent positive cells as determined by QuPath digital image analysis are shown as box plots for 23 paired core biopsy samples, which were analyzed both on whole slide IHC biopsies (left) and as microcores on TMA (right). The corresponding samples are connected by lines (red and blue for samples positive and negative based on RNA-seq, respectively). Although for six samples, higher percentages of positive cells were obtained in TMA analysis; for 11 (64.7%) of the positive samples, the expression signal was lost in TMA analysis because of a drop below the 10% cutoff.

remained as significant independent predictor for pCR in this analysis showing a significant interaction with bevacizumab treatment ($P = 0.020$ and 0.021, respectively).

Validation of the predictive hypoxia signature by IHC

We selected NDRG1 as single marker for the hypoxia signature based on good correlation ($R^2 = 0.526$) of IHC and mRNA in an independent microarray dataset (ref. 17; see Supplementary Fig. S2A; Materials and Methods section, for details). We next tested whether NDRG1 IHC can be performed on core biopsy samples from GeparQuinto (Supplementary Fig. S2B). We used a cutoff of z-score 1.5 from the RNA-seq data as strong expression and selected a test cohort of 27 GeparQuinto samples for whole slide IHC of core biopsies (Supplementary Fig. S2B). Blinded visual scoring of 23 evaluable samples showed high sensitivity (89.5%) and specificity (100%) in this finding cohort (Supplementary Table S6). When we applied digital image analysis (46), a cutoff of 10% positive cells led to a sensitivity of 68.4% and specificity of 100% compared with RNA-seq (Supplementary Table S6). Finally, we analyzed a TMA cohort of small microcores from the core biopsies of 251 GeparQuinto samples with RNA-seq data using digital image analysis (Supplementary Fig. S2C; Materials and Methods section). We expected critical challenges for reliable detection of the heterogenous expression in the tiny TMA cores from the trial. Nevertheless, we observed a significant predictive value for pCR when we used the z-score of the percentage of positive cells from digital image analysis of the TMA samples in univariate logistic regression (OR = 1.36; 95% CI, 1.04–1.79; $P = 0.025$). In contrast, in multivariate analysis using z-score 1.5 as cutoff we detected only a nonsignificant trend (OR = 3.79; 95% CI, 0.85–16.9; $P = 0.080$; Supplementary Table S10). We suspected that the reduced predictive value in this analysis is due to loss of the heterogeneous expression signal in the small microcore tissue samples of the TMA. Therefore, we also compared results of digital image analyses from whole slide IHC of core biopsies and from microcores of the TMA in the finding cohort of 23 samples. For this, we applied the cutoff of 10% positive cells described previously. We then calculated sensitivity and specificity of the image analyses of whole slide and TMA based on the RNA-seq data cutoff z-score 1.5. We found a considerable drop in sensitivity from 68.4% to 36.8% on TMA slides (Supplementary Table S6; **Figs. 2** and **3**). Finally, we compared RNA-seq and TMA results of all 193 samples with high-quality RNA-seq, and also observed a low sensitivity of only 40.0%. Moreover, the PPV was only 25.8% among those 193 samples because 23 with more than 10% positive cells had an RNA-seq z-score below 1.5 (Supplementary Table S6; Supplementary Fig. S7). These results demonstrate that a reliable detection of the hypoxia signature may only be feasible on whole slide IHC of core biopsies.

Discussion

We have previously shown that hypoxia/inflammatory signatures (VEGFA/IL8 metagenes) are associated with poor prognosis in TNBC (17, 18). Hypoxia in the tumor can induce an immunosuppressive microenvironment and several studies have demonstrated the benefit of combining anti-VEGF agents with various immunotherapies, already leading to FDA approval in kidney cancer (13–16). On the other hand, hypoxia is an important regulator of VEGF (11) and it may also be hypothesized that hypoxic tumors could be more dependent on VEGF and more responsive to its inhibition. Another simplistic model could be that hypoxia and necrosis signatures might characterize tumors that are already "knocked on," and such tumors may show increased response to different kinds of treatment. Therefore, we tested the predictive value of our small hypoxia signature for pCR after bevacizumab in samples from the neoadjuvant Geparquinto trial according to a prespecified protocol in a blinded fashion.

Our study demonstrates first, that exome-capture RNA-seq allows robust subtyping of clinical samples with limited FFPE tissue from neoadjuvant core biopsies. We found strong agreement of molecular and pathologic parameters, as for example, hormone receptor status, histologic grading, and lymphocyte infiltration, and verified the known differences in pCR rates between molecular subtypes. Second, in prespecified analyses we found that several signatures (molecular subtype, proliferation, T cell, and hypoxia signatures) significantly predicted pCR (Supplementary Table S9). Strikingly, the hypoxia signature remained significant in a multivariate model of pCR and showed a significant interaction with bevacizumab treatment (**Table 2**). In patients without bevacizumab treatment, we only observed a nonsignificant trend for pCR in univariate analysis (OR = 1.40; 95% CI = 0.97–2.02; $P = 0.076$; Supplementary Fig. S8), which may suggest also an increased sensitivity to chemotherapy of tumors with high hypoxia signature.

Our IHC studies suggest that the cellular source of the hypoxia RNA-signature are perinecrotic cells. Highly heterogenous expression within tissue precluded a reliable IHC detection in the tiny TMA microcores from the core biopsies of the trial (**Figs. 2** and **3**). Even if we could still detect a predictive value for pCR, this heterogeneity led to a tremendous loss of sensitivity and specificity (Supplementary Table S6). Therefore, whole slide IHC is required for reliable detection and further study of the hypoxia signature. On the other hand, because necrosis detection in routine pathology is straight forward, we suggest that estimating and reporting the amount of necrosis in the pathology report may also be helpful in predicting response to chemotherapy, and could potentially be useful as stratification factor in clinical trials.

Several other biomarker for bevacizumab response has been proposed and it is becoming clear that single markers may not be sufficient to predict complex phenotypes as the response to bevacizumab (10). Thus, future studies may integrate individual effects of different markers from tissue and plasma using advanced statistical analyses and combination into general predictive scores, which may allow more robust predictions across cancers (10). These may also include important information of changes during treatment that have been reported (11, 49). Moreover, the role of a marker may also depend on treatment combinations. For example, in our study hypoxia seems to predict response to bevacizumab and chemotherapy. But on the other hand, hypoxia seems to induce an immunosuppressive microenvironment (15) and therefore could also have a potential role as predictive factor for immunotherapy and for combinations of bevacizumab with checkpoint inhibitors (14, 16).

Despite improvement of pCR bevacizumab did not increase breast cancer survival in several studies, which might be due to a greater effect on vascularization of the primary tumor than on micrometastases (6–8). The hypoxia signature has been associated with poor survival in TNBC (17, 18) and metastasis in different tumor types (33). However, we could not detect a prognostic value of the signature for long term survival in the GeparQuinto trial patients (data not shown), but our RNA-Seq dataset was clearly not sufficiently powered for such analyses.

Strenghts of our study are, first that we used samples from a randomized controlled trial, second that we prospectively developed an SAP and followed a pre-specified blinded protocol, and third that we tested only a limited number of pre-specified variables thereby avoiding problems of multiple testing. However, our study has limitations. First, only a subset of patients from the trial was included and the availability of tissue samples could introduce bias. In particular, we included all available tissue samples from HER2 negative patients with pCR. Because of this enrichment in pCR patients, there were also more hormone receptor negative high grade tumors in the RNA-Seq analyses set (Supplementary Table S3). Nevertheless, we did not enrich for pCR cases in the immunohistochemical validation on TMA, but still observed a predictive effect of the marker for pCR in that data. Second, despite our RNA-Seq dataset represents the largest so far for breast cancers with neoadjuvant bevacizumab treatment, the sample size is still very small, as even the complete GeparQuinto trial was not powered for survival differences. Finally, a proper validation RNA-Seq dataset for our findings is yet missing.

In conclusion, our study shows that exome-capture RNA-Seq allows robust genomic characterization of clinical samples with limited FFPE material from core biopsies and the derived molecular subtypes and immune signatures are predictive for pCR. We found that a small hypoxia signature specifically predicts pCR to bevacizumab treatment, which could be validated by immunohistochemical analysis. The signature may have important applications as predictive factor for bevacizumab response in different cancer types, as well as for novel combination treatments of bevacizumab with immune checkpoint inhibition (13–16).

Disclosure of Potential Conflicts of Interest

K.E. Weber holds ownership interest (including patents) in Sividon Diagnostics, EndoPredict, patent PCT/EP2019/083124, and is listed as a co-inventor on a provisional patent application on prognostic or predictive biomarkers for cancer immunotherapy that is owned by German Breast Group Forschungs GmbH, Charité-Universitätsmedizin Berlin, and Goethe Universität Frankfurt. C. Denkert is an employee/paid consultant for MSD Oncology, Amgen, and Daiichi Sankyo, reports receiving speakers bureau honoraria from Teva, Roche, Novartis, Pfizer, and Amgen, and holds ownership interest (including patents) in Sividon Diagnostics. P.A. Fasching is an employee/paid consultant for Novartis, Roche, Pfizer, Celgene, Daiichi-Sankyo, Pierre Fabre, Astra Zeneca, Merck Sharp & Dohme, Eisai, and Lilly, reports receiving commercial research grants from Biontech and Cepheid, and is an advisory board member/unpaid consultant for Novartis. V. Müller is an employee/paid consultant for Genomic Health, Hexal, Roche, Pierre Fabre, Amgen, ClinSol, Novartis, MSD, Daiichi-Sankyo, Eisai, Lilly, Tesaro and Nektar, reports receiving commercial research grants from Roche and Genentech, and speakers bureau honoraria from Amgen, Astra Zeneca, Celgene, Daiichi-Sankyo, Eisai, Pfizer, MSD, Novartis, Roche, and Teva. C. Hanusch reports receiving speakers bureau honoraria from Roche, Novartis, Celgene, Pfizer, Lilly, Astra Zeneca, and Amgen. J. Huober reports receiving commercial research grants from Novartis, Celgene, and Hexal, speakers bureau honoraria from Lilly, Novartis, Roche, Pfizer, Astra Zeneca, Merck Sharp & Dhome, Celgene, Eisai, and Abbvie, and is an advisory board member/unpaid consultant for Lilly, Novartis, Roche, Astra Zeneca, Celgene, Abbvie, Merck Sharp & Dhome, and Hexal. M. van Mackelenbergh reports receiving speakers bureau honoraria from Amgen, AstraZeneca, and GenomicHealth, and other remuneration from Novartis and Lilly. B. Leyland-Jones is an employee/paid consultant for NedBiosystems, and reports receiving speakers bureau honoraria from Genentech, Bayer, Exelixis, and Puma. T. Fehm is an employee/paid consultant for Novartis, Roche, Pfizer, Daichii Sankyo, and Celgene. S. Loibl is an employee/paid consultant for GBG Forschungs GmbH. No potential conflicts of interest were disclosed by the other authors.

Role of the Funder

The funding sources had no roles in the design and conduct of the study; collection, management, analysis, and interpretation of the data; preparation, review, or approval of the manuscript; and decision to submit the manuscript for publication.

Authors' Contributions

Conception and design: T. Karn, T. Meissner, K.E. Weber, C. Denkert, B. Gerber, C. Hanusch, M. Untch, S. Loibl

Development of methodology: T. Karn, B. Gerber, M. Untch, S. Loibl

Acquisition of data (provided animals, acquired and managed patients, provided facilities, etc.): T. Karn, T. Meissner, C. Solbach, C. Denkert, K. Engels, P.A. Fasching, B.V. Sinn, I. Schrader, J. Budczies, V. Müller, B. Gerber, C. Schem, B.M. Young, C. Hanusch, J. Huober, B. Leyland-Jones, T. Fehm, V. Nekljudova, S. Loibl

Analysis and interpretation of data (e.g., statistical analysis, biostatistics, computational analysis): T. Karn, T. Meissner, K.E. Weber, U. Holtrich, B. Gerber, M. Untch

Writing, review, and/or revision of the manuscript: T. Karn, T. Meissner, K.E. Weber, C. Solbach, C. Denkert, K. Engels, P.A. Fasching, B.V. Sinn, J. Budczies, F. Marmé, V. Müller, U. Holtrich, B. Gerber, C. Schem, C. Hanusch, E. Stickeler, J. Huober, M. van Mackelenbergh, B. Leyland-Jones, T. Fehm, V. Nekljudova, M. Untch, S. Loibl

Administrative, technical, or material support (i.e., reporting or organizing data, constructing databases): T. Karn, K.E. Weber, M. Untch, S. Loibl

Study supervision: T. Karn, I. Schrader

Acknowledgments

This work was supported by grants from the H.W. & J. Hector-Stiftung, Mannheim, Germany (M82 to U. Holtrich and T. Karn); and the Avera McKennan Hospital & University Health Center and Avera McKennan Foundation. The authors would like to thank all patients, clinicians, and pathologists for participating in the GeparQuinto trial and the staff of the German Breast Group for their help coordinating samples and clinical information and support in this translational research project.

The costs of publication of this article were defrayed in part by the payment of page charges. This article must therefore be hereby marked *advertisement* in accordance with 18 U.S.C. Section 1734 solely to indicate this fact.

Received June 18, 2019; revised November 19, 2019; accepted January 8, 2020; published first January 13, 2020.

Published OnlineFirst January 13, 2020; DOI: 10.1158/1078-0432.CCR-19-1954

References

1. Minckwitz G von, Eidtmann H, Rezai M, Fasching PA, Tesch H, Eggemann H, et al. Neoadjuvant chemotherapy and bevacizumab for HER2-negative breast cancer. N Engl J Med 2012;366:299–309.
2. Bear HD, Tang G, Rastogi P, Geyer CE, Robidoux A, Atkins JN, et al. Bevacizumab added to neoadjuvant chemotherapy for breast cancer. N Engl J Med 2012;366:310–20.
3. Earl HM, Hiller L, Dunn JA, Blenkinsop C, Grybowicz L, Vallier A-L, et al. Efficacy of neoadjuvant bevacizumab added to docetaxel followed by fluorouracil, epirubicin, and cyclophosphamide, for women with HER2-negative early breast cancer (ARTemis): an open-label, randomised, phase 3 trial. Lancet Oncol. 2015;16:656–66.
4. Nahleh ZA, Barlow WE, Hayes DF, Schott AF, Gralow JR, Sikov WM, et al. SWOG S0800 (NCI CDR0000636131): addition of bevacizumab to neoadjuvant nab-paclitaxel with dose-dense doxorubicin and cyclophosphamide improves pathologic complete response (pCR) rates in inflammatory or locally advanced breast cancer. Breast Cancer Res Treat 2016;158:485–95.
5. Cameron D, Brown J, Dent R, Jackisch C, Mackey J, Pivot X, et al. Adjuvant bevacizumab-containing therapy in triple-negative breast cancer (BEATRICE): primary results of a randomised, phase 3 trial. Lancet Oncol. 2013;14:933–42.
6. Minckwitz G von, Loibl S, Untch M, Eidtmann H, Rezai M, Fasching PA, et al. Survival after neoadjuvant chemotherapy with or without bevacizumab or everolimus for HER2-negative primary breast cancer (GBG 44-GeparQuinto)†. Ann Oncol 2014;25:2363–72.
7. Bear HD, Tang G, Rastogi P, Geyer CE, Liu Q, Robidoux A, et al. Neoadjuvant plus adjuvant bevacizumab in early breast cancer (NSABP B-40 NRG Oncology): secondary outcomes of a phase 3, randomised controlled trial. Lancet Oncol. 2015;16:1037–48.
8. Earl HM, Hiller L, Dunn J, Blenkinsop C, Grybowicz L, Vallier A-L, et al. Disease-free and overall survival at 3.5 years for neoadjuvant bevacizumab added to docetaxel followed by fluorouracil, epirubicin and cyclophosphamide, for women with HER2 negative early breast cancer: ARTemis Trial. Ann. Oncol. 2017;28:1817–24.
9. Pusztai L, Szekely B, Hatzis C. Is complete response the answer? Ann. Oncol. 2017;28:1681–83.
10. Lambrechts D, Lenz H-J, Haas S de, Carmeliet P, Scherer SJ. Markers of response for the antiangiogenic agent bevacizumab. J Clin Oncol 2013;31:1219–30.
11. Jubb AM, Harris AL. Biomarkers to predict the clinical efficacy of bevacizumab in cancer. Lancet Oncol. 2010;11:1172–83.
12. Roviello G, Bachelot T, Hudis CA, Curigliano G, Reynolds AR, Petrioli R, et al. The role of bevacizumab in solid tumours: a literature based meta-analysis of randomised trials. Eur J Cancer 2017;75:245–58.
13. Socinski MA, Jotte RM, Cappuzzo F, Orlandi F, Stroyakovskiy D, Nogami N, et al. Atezolizumab for first-line treatment of metastatic nonsquamous NSCLC. N Engl J Med 2018;378:2288–301.
14. McDermott DF, Huseni MA, Atkins MB, Motzer RJ, Rini BI, Escudier B, et al. Clinical activity and molecular correlates of response to atezolizumab alone or in combination with bevacizumab versus sunitinib in renal cell carcinoma. Nat Med 2018;24:749–57.
15. Fukumura D, Kloepper J, Amoozgar Z, Duda DG, Jain RK. Enhancing cancer immunotherapy using antiangiogenics: opportunities and challenges. Nat Rev Clin Oncol 2018;15:325–40.
16. Munn LL, Jain RK.Vascular regulation of antitumor immunity. Science 2019;365:544–45.
17. Rody A, Karn T, Liedtke C, Pusztai L, Ruckhaeberle E, Hanker L, et al. A clinically relevant gene signature in triple negative and basal-like breast cancer. Breast Cancer Res 2011;13:R97.
18. Karn T, Jiang T, Hatzis C, Sänger N, El-Balat A, Rody A, et al. Association between genomic metrics and immune infiltration in triple-negative breast cancer. JAMA Oncol 2017;3:1707–11.
19. Cieslik M, Chugh R, Wu Y-M, Wu M, Brennan C, Lonigro R, et al. The use of exome capture RNA-seq for highly degraded RNA with application to clinical cancer sequencing. Genome Res 2015;25:1372–81.
20. Priedigkeit N, Watters RJ, Lucas PC, Basudan A, Bhargava R, Horne W, et al. Exome-capture RNA sequencing of decade-old breast cancers and matched decalcified bone metastases. JCI Insight 2017;2: pii: 95703.
21. McShane LM, Altman DG, Sauerbrei W, Taube SE, Gion M, Clark GM. Reporting recommendations for tumor marker prognostic studies. J Clin Oncol 2005;23:9067–72.
22. Simon RM, Paik S, Hayes DF. Use of archived specimens in evaluation of prognostic and predictive biomarkers. J. Natl. Cancer Inst. 2009;101:1446–52.
23. Moher D, Schulz KF, Altman D. The CONSORT statement: revised recommendations for improving the quality of reports of parallel-group randomized trials. JAMA 2001;285:1987–91.
24. Zhao W, He X, Hoadley KA, Parker JS, Hayes DN, Perou CM. Comparison of RNA-Seq by poly (A) capture, ribosomal RNA depletion, and DNA microarray for expression profiling. BMC Genom. 2014;15:419.
25. Cabanski CR, Magrini V, Griffith M, Griffith OL, McGrath S, Zhang J, et al. cDNA hybrid capture improves transcriptome analysis on low-input and archived samples. J Mol Diagn 2014;16:440–51.
26. Schuierer S, Carbone W, Knehr J, Petitjean V, Fernandez A, Sultan M, et al. A comprehensive assessment of RNA-seq protocols for degraded and low-quantity samples. BMC Genom 2017;18:442.
27. Fisch KM, Meißner T, Gioia L, Ducom J-C, Carland TM, Loguercio S, et al. Omics Pipe: a community-based framework for reproducible multi-omics data analysis. Bioinformatics 2015;31:1724–28.
28. Dobin A, Davis CA, Schlesinger F, Drenkow J, Zaleski C, Jha S, et al. STAR: ultrafast universal RNA-seq aligner. Bioinformatics 2013;29:15–21.
29. Liao Y, Smyth GK, Shi W. featureCounts: an efficient general purpose program for assigning sequence reads to genomic features. Bioinformatics 2014;30:923–30.
30. Love MI, Huber W, Anders S. Moderated estimation of fold change and dispersion for RNA-seq data with DESeq2. Genome Biol 2014;15:550.
31. Karn T, Metzler D, Ruckhäberle E, Hanker L, Gätje R, Solbach C, et al. Data-driven derivation of cutoffs from a pool of 3,030 Affymetrix arrays to stratify distinct clinical types of breast cancer. Breast Cancer Res Treat 2010;120:567–79.
32. Paquet ER, Hallett MT. Absolute assignment of breast cancer intrinsic molecular subtype. J. Natl. Cancer Inst. 2015;107:357.
33. Hu Z, Fan C, Livasy C, He X, Oh DS, Ewend MG, et al. A compact VEGF signature associated with distant metastases and poor outcomes. BMC medicine 2009;7:9.
34. Curtis C, Shah SP, Chin S-F, Turashvili G, Rueda OM, Dunning MJ, et al. The genomic and transcriptomic architecture of 2,000 breast tumours reveals novel subgroups. Nature 2012;486:346–52.
35. Comprehensive molecular portraits of human breast tumours. Nature 2012;490:61–70.
36. Perou CM, Sørlie T, Eisen MB, van de Rijn M, Jeffrey SS, Rees CA, et al. Molecular portraits of human breast tumours. Nature 2000;406:747–52.
37. Wirapati P, Sotiriou C, Kunkel S, Farmer P, Pradervand S, Haibe-Kains B, et al. Meta-analysis of gene expression profiles in breast cancer: toward a unified understanding of breast cancer subtyping and prognosis signatures. Breast Cancer Res 2008;10:R65.
38. Desmedt C, Haibe-Kains B, Wirapati P, Buyse M, Larsimont D, Bontempi G, et al. Biological processes associated with breast cancer clinical outcome depend on the molecular subtypes. Clin Cancer Res 2008;14:5158–65.
39. Karn T, Pusztai L, Holtrich U, Iwamoto T, Shiang CY, Schmidt M, et al. Homogeneous datasets of triple negative breast cancers enable the identification of novel prognostic and predictive signatures. PLoS One 2011;6:e28403.
40. Buffa FM, Harris AL, West CM, Miller CJ. Large meta-analysis of multiple cancers reveals a common, compact and highly prognostic hypoxia metagene. Br J Cancer 2010;102:428–35.
41. Weiler M, Blaes J, Pusch S, Sahm F, Czabanka M, Luger S, et al. mTOR target NDRG1 confers MGMT-dependent resistance to alkylating chemotherapy. PNAS 2014;111:409–14.
42. Zhang P, Tchou-Wong K-M, Costa M. Egr-1 mediates hypoxia-inducible transcription of the NDRG1 gene through an overlapping Egr-1/Sp1 binding site in the promoter. Cancer Res 2007;67:9125–33.
43. Tanaka K, Babic I, Nathanson D, Akhavan D, Guo D, Gini B, et al. Oncogenic EGFR signaling activates an mTORC2-NF-κB pathway that promotes chemotherapy resistance. Cancer Discov 2011;1:524–38.
44. Verma N, Müller A-K, Kothari C, Panayotopoulou E, Kedan A, Selitrennik M, et al. Targeting of PYK2 synergizes with EGFR antagonists in basal-like TNBC

Published OnlineFirst January 13, 2020; DOI: 10.1158/1078-0432.CCR-19-1954

and circumvents HER3-associated resistance via the NEDD4-NDRG1 axis. Cancer Res 2017;77:86–99.
45. Ellen TP, Ke Q, Zhang P, Costa M. NDRG1, a growth and cancer related gene: regulation of gene expression and function in normal and disease states. Carcinogenesis 2008;29:2–8.
46. Bankhead P, Loughrey MB, Fernández JA, Dombrowski Y, McArt DG, Dunne PD, et al. QuPath: open source software for digital pathology image analysis. Sci Rep 2017;7:16878.
47. Loughrey MB, Bankhead P, Coleman HG, Hagan RS, Craig S, McCorry AMB, et al. Validation of the systematic scoring of immunohistochemically stained tumour tissue microarrays using QuPath digital image analysis. Histopathology 2018;73:327–38.
48. Issa-Nummer Y, Darb-Esfahani S, Loibl S, Kunz G, Nekljudova V, Schrader I, et al. Prospective validation of immunological infiltrate for prediction of response to neoadjuvant chemotherapy in HER2-negative breast cancer—a substudy of the neoadjuvant GeparQuinto trial. PLoS One 2013;8:e79775.
49. Höglander EK, Nord S, Wedge DC, Lingjærde OC, Silwal-Pandit L, Gythfeldt Hv, et al. Time series analysis of neoadjuvant chemotherapy and bevacizumab-treated breast carcinomas reveals a systemic shift in genomic aberrations. Genome Med 2018;10:92.

AACR American Association for Cancer Research

Clinical Cancer Research

A Small Hypoxia Signature Predicted pCR Response to Bevacizumab in the Neoadjuvant GeparQuinto Breast Cancer Trial

Thomas Karn, Tobias Meissner, Karsten E. Weber, et al.

Clin Cancer Res Published OnlineFirst January 13, 2020.